Supplementary Table 1. Primer sequences used for qPCR.

Target	Forward Sequence 5'→3'	Reverse Sequence 5'→3'	Ref.
Universal 16S	ACTCCTACGGGAGGCAGCAGT	ATTACCGCGGCTGCTGGC	[45]
Enterobacteriaceae Family	GTGCCAGCAGCCGCGGTAA	GCCTCAAGGGCACAACCTCCAAG	[45]
Clostridiales Order	ACTCCTACGGGAGGCAGC	GCTTCTTAGTCAGGTACCGTCAT	[45]
Lactobacillaceae Family	AGCAGTAGGGAATCTTCCA	CACCGCTACACATGGAG	[45]
Enterococcus Family	CCCTTATTGTTAGTTGCCATCATT	ACTCGTTGTACTTCCCATTGT	[45]
Bacteroidetes Class	AGCAGCCGCGGTAAT	GCATTTCACCGCTA	[45]
B. thetaiotamicron 16S	CCCGATGGTATAATCAGAC	CACAACTGACTTAACTGTCC	[46]
B. fragilis 16S	TGATTCCGCATGGTTTCATT	CGACCCATAGAGCCTTCATC	[46]
Actin	GCACTCTTCCAGCCTTCCTTCC	CAGGTCTTTGCGGATGTCCACG	[29]
SOCS3	GGCCACTCTTCAGCATCTC	ATCGTACTGGTCCAGGAACTC	[29]
CLDN1	CCAGTCAATGCCAGGTACGAAT	TTGGTGTTGGGTAAGAGGTTGTT	[47]
CLDN2	CTCCTGGGATTCATTCCTGTT	TCAGGCACCAGTGGTGAGTAGA	[47]
CLDN4	GGCTGCTTTGCTGCAAC	AGAGCGGGCAGCAGAATACTT	[47]
MUC2	GTAAGAAGTGTGAACAGACG	AGAATGTGCAGTTGTTCTTC	

Figure S1

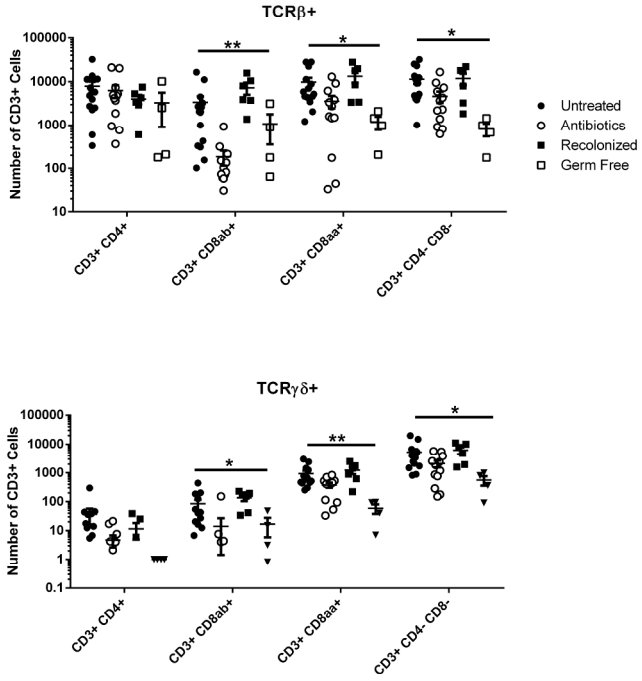

Figure S1. Antibiotics reversibly alter colon IEL numbers and phenotype. Groups of 3-9 C57Bl/6 mice aged 8-12 weeks were untreated, treated with antibiotics for one week, or treated with antibiotics for one week followed by cohousing with untreated littermates for recolonization. Data are from two independent experiments. The absolute number of IELs was quantified by flow cytometry. Each dot represents an individual mouse and the bars represent the mean ± SEM. A one-way ANOVA with Dunnett's post-test analysis was used to determine statistical significance. *, $P<0.05$; **, $P<0.01$

215x279mm (300 x 300 DPI)

Figure S2

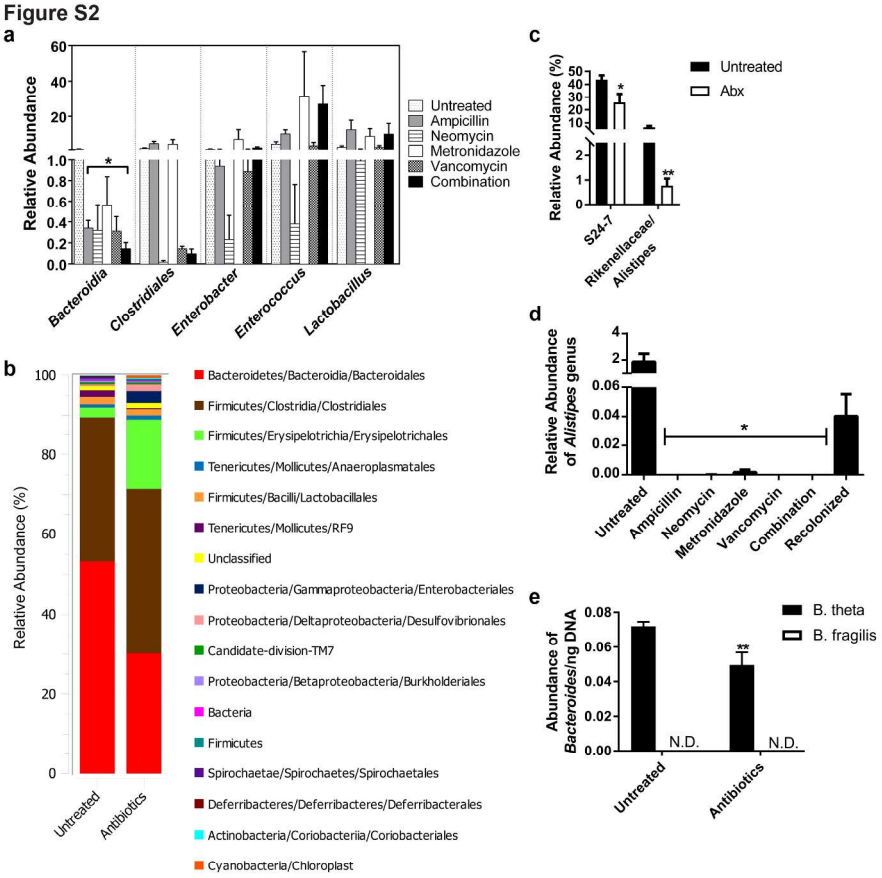

Figure S2. Effect of antibiotic treatment on fecal microbiome in mice. (a) Fecal DNA harvested from pellets from untreated and antibiotic-treated mice was analyzed by qPCR for Bacteroidia class, Clostridiales order, Enterobacteriaceae family, Enterococcus family, and Lactobacillaceae family specific 16S DNA and normalized to a universal bacterial 16S primer set. Data are shown as the mean relative abundance compared to untreated mice within the specific primer set ± SEM. *, P<0.05 as determined by the Kruskall-Wallis test with Dunn's post-test. (b,c) Fecal DNA from 5 untreated and 5 antibiotic-treated C57Bl/6 mice was harvested and the 16S rRNA sequenced. (b) The percent abundance of OTUs at the order level representing at least 1% of the total bacterial population in either group are shown. (c) Using a Wilcoxon rank test, the most significant OTU changes within Bacteroidiales were identified and shown as the mean relative abundance ± SEM. *, P<0.05; **, P<0.01. (d) Fecal DNA was analyzed by qPCR for Alistipes genus specific 16S DNA and normalized to a universal bacterial 16S primer set. Data are shown as the mean relative abundance compared to untreated mice ± SEM. *, P<0.05 as determined by the Kruskall-Wallis test with Dunn's post-test. (e) Abundance of B. thetaiotamicron (abbreviated as B. theta) and B. fragilis were determined by qPCR and shown as the mean ± SEM. A Mann-Whitney test demonstrated statistical significance. **, P<0.01. N.D.=not detected.

215x279mm (300 x 300 DPI)

Figure S3

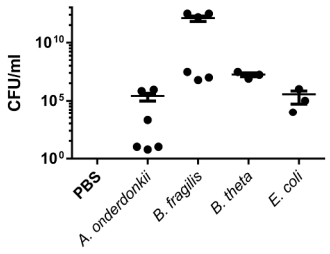

Figure S3. Bacterial spp. colonization of germ free mice. 8-12 week old C57Bl6 germ free mice were gavaged with 1.5-3 X 10^9 CFU/ml of A. onderdonkii or B. fragilis. After two weeks, colonization was confirmed by culture of cecal contents. Each dot represents the colonization level in an individual mouse and the bars are the mean ± SEM. Data are from two independent experiments of 3 mice per group.

215x279mm (300 x 300 DPI)

Figure S4

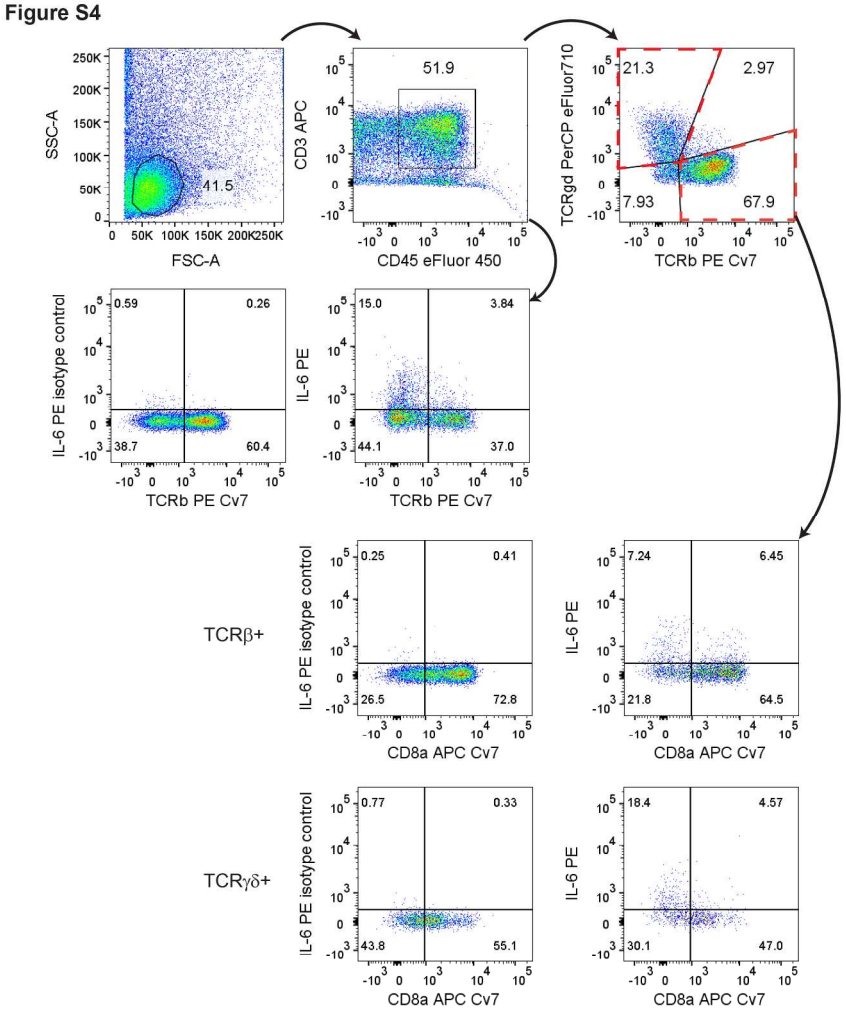

Figure S4. IL-6 production by IELs. IELs were harvested from the colons of C57Bl/6 mice, magnetically sorted, and mitogen-stimulated for two hours in the prescence of protein transport blockers. Cells were then stained for T cell surface markers followed by fixation and permeabilization for intracellular staining for IL-6 or isotype control. Representative dot plots are shown for the gating strategy for T cells and IL-6 positivity in the TCR+ subsets CD8α- vs. CD8α+.

215x279mm (300 x 300 DPI)

Figure S5

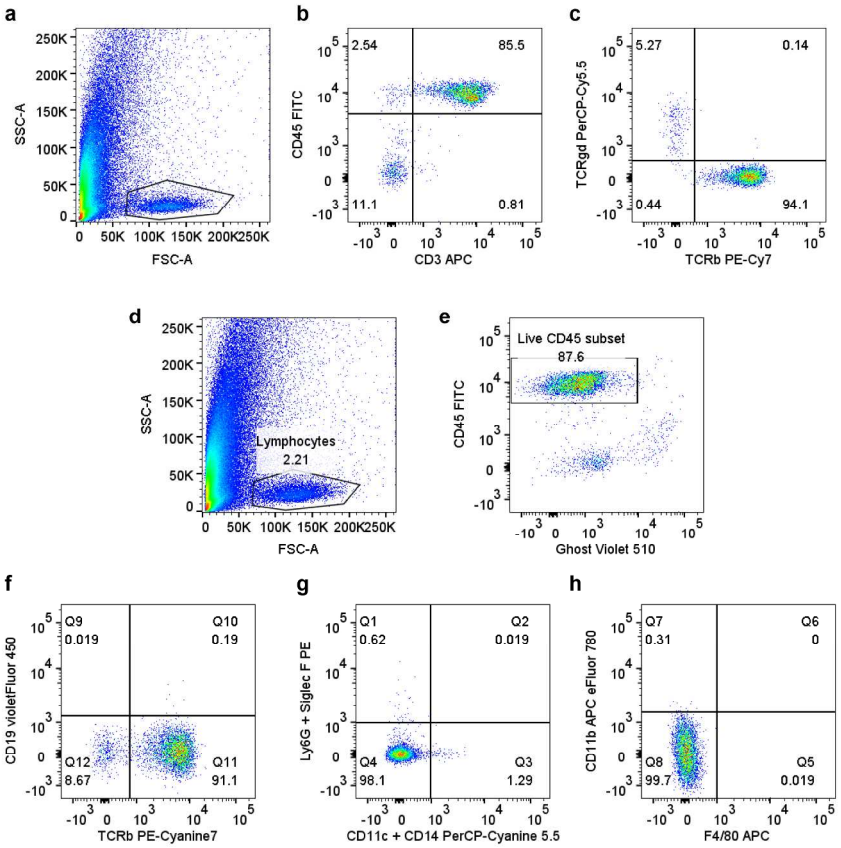

Figure S5. Magnetic sorting of IELs. Following EDTA-liberation of epithelial cells, IELs were magnetically purified using negative selection as described in Methods. Purity of the sorted cells was verified by flow cytometry. Representative plots are shown. (a, d) Immune cells were gated based on forward and side scatter properties. (b) Gated lymphocytes were assessed for CD45+ CD3+ cells that were then (c) evaluated for the presence of a TCR. (e) Viable CD45+ cells were evaluated for the presence of (f) CD19 versus TCRb, (g) Ly6G, Siglec F, CD11c, and CD14, and (h) CD11b and F4/80.

215x279mm (300 x 300 DPI)

Figure S6

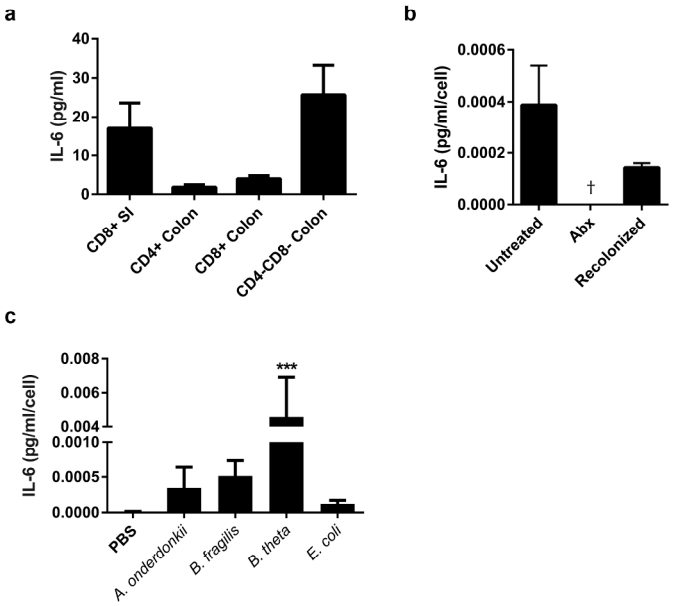

Figure S6. IL-6 secretion by IELs is dependent upon an intact microbiota. 8-12 week old C57Bl/6 mice were untreated, antibiotic-treated, or recolonized after antibitocs. IELs were harvested from these mice, magnetically sorted, and mitogen-stimulated. IL-6 in the culture supernatant was measured by ELISA. (a) IL-6 production by IEL subsets. (b) IL-6 normalized to the total number of IELs harvested from the colons. † = no meaningful value could be determined for this group. (c) Normalized IL-6 in monocolonized germ free mice. Data are the ± SEM; an one-way ANOVA with Dunnett's test determined signficance with *, $P<0.05$ and ***, $P<0.001$.

215x279mm (300 x 300 DPI)

Figure S7

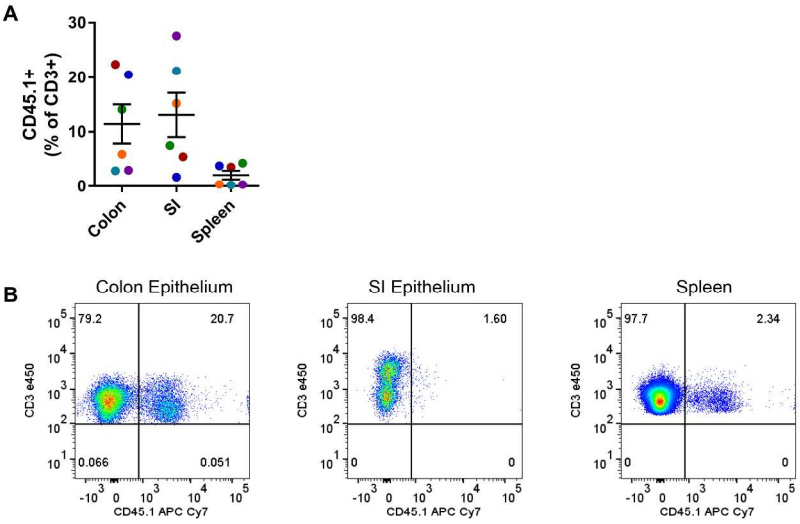

Figure S7. Transfer of colonic IELs traffic back to the intestine. Donor CD45.1 IELs were harvested, magnetically sorted, and 1-2 x 10^5 labeled cells were injected IV into C57Bl/6 (CD45.2+) wild type recipient mice. After one week, cells from the colon epithelium, SI epithelium, and spleen were harvested from the recipient mice and evaluated for the presence of CD45.1 donor cells by flow cytometry. (A) Each dot represents the percentage of donor (CD45.1) CD3+ cells in the total IEL population from the recipient mice. Each color represents an individual mouse's data fro the tissues shown. Bars are the mean ± SEM. (B) Representative FACS plots for the tissues specified from an individual mouse are shown. The plots shown are after gating on viable lymphocytes based on FSC, SSC, and absence of ghost dye stain.

215x279mm (300 x 300 DPI)